0026-895X/03/6406-1283–1294$7.00
MOLECULAR PHARMACOLOGY
Copyright © 2003 The American Society for Pharmacology and Experimental Therapeutics
Mol Pharmacol 64:1283–1294, 2003

Vol. 64, No. 6
2676/1105149
Printed in U.S.A.

Characterization of Human $\alpha4\beta2$-Nicotinic Acetylcholine Receptors Stably and Heterologously Expressed in Native Nicotinic Receptor-Null SH-EP1 Human Epithelial Cells

J. BREK EATON, JIAN-HONG PENG, KATHERINE M. SCHROEDER, ANDREW A. GEORGE, JOHN D. FRYER,[1] CHANDRA KRISHNAN, LORI BUHLMAN, YEN-PING KUO, ORTRUD STEINLEIN, and RONALD J. LUKAS

Division of Neurobiology, Barrow Neurological Institute, Phoenix, Arizona (J.B.E., J.-H.P., K.M.S., A.A.G., J.D.F., C.K., L.B., Y.-P.K., R.J.L.); and Institute for Human Genetics, Rheinische Friedrich-Wilhelms-Universitat, Bonn, Germany (O.S.)

Received May 21, 2003; accepted July 30, 2003

This article is available online at http://molpharm.aspetjournals.org

ABSTRACT

Naturally expressed nicotinic acetylcholine receptors composed of $\alpha4$ and $\beta2$ subunits ($\alpha4\beta2$-nAChR) are the predominant form of high affinity nicotine binding site in the brain implicated in nicotine reward, mediation of nicotinic cholinergic transmission, modulation of signaling through other chemical messages, and a number of neuropsychiatric disorders. To develop a model system for studies of human $\alpha4\beta2$-nAChR allowing protein chemical, functional, pharmacological, and regulation of expression studies, human $\alpha4$ and $\beta2$ subunits were stably introduced into the native nAChR-null human epithelial cell line SH-EP1. Heterologously expressed $\alpha4\beta2$-nAChR engage in high-affinity, specific binding of ^{3}H-labeled epibatidine (H-EBDN; macroscopic K_D = 10 pM; k_{on} = 0.74/min/nM, k_{off} = 0.013/min). Immunofluorescence studies show $\alpha4$ and $\beta2$ subunit protein expression in virtually every transfected cell, and microautoradiographic studies show expression of ^{125}I-labeled iodo-deschloro-epibatidine binding sites in most cells. H-EBDN binding competition studies reveal high affinity for nicotinic agonists and lower affinity for nicotinic antagonists. Heterologously expressed $\alpha4\beta2$-nAChR functional studies using $^{86}Rb^{+}$ efflux assays indicate full efficacy of epibatidine, nicotine, and acetylcholine; partial efficacy for 1,1-dimethyl-4-phenyl-piperazinium, cytisine, and suberyldicholine; competitive antagonism by dihydro-β-erythroidine, decamethonium, and methyllycaconitine; noncompetitive antagonism by mecamylamine and eserine; and mixed antagonism by pancuronium, hexamethonium, and *d*-tubocurarine. These results demonstrate utility of transfected SH-EP1 cells as models for studies of human $\alpha4\beta2$-nAChR, and they also reveal complex relationships between apparent affinities of drugs for radioligand binding and functional sites on human $\alpha4\beta2$-nAChR.

Nicotinic acetylcholine receptors (nAChR) are prototypical members of the ligand-gated ion channel superfamily of neurotransmitter receptors (see reviews and/or tables by Lindstrom, 1996; Lukas, 1998; Lukas et al., 1999; Clementi et al., 2000; Alexander and Peters, 2001). nAChR represent both classic and contemporary models for the establishment of concepts pertaining to mechanisms of drug action, synaptic transmission, and structure and function of transmembrane signaling molecules. nAChR found postsynaptically on muscle, postganglionic neurons, or central neurons mediating depolarizing, inward Na^{+} currents play important roles in classic excitatory neurotransmission. nAChR on motor, preganglionic, or central neuronal terminals also can modulate neurotransmitter release. nAChR exist as a diverse family of molecules composed of different combinations of subunits derived from at least 17 genes ($\alpha1$–$\alpha10$, $\beta1$–$\beta4$, γ, δ, ϵ; see reviews cited above and Elgoyhen et al., 2001). Naturally expressed nAChR in muscle are made from $\alpha1$, $\beta1$, δ, and either γ (fetal) or ϵ (adult) subunits and have properties just like those of heterologously expressed nAChR made of the same subunits. nAChR can form as homomers of the most ancient nAChR subunits, $\alpha7$, $\alpha8$, or $\alpha9$, although $\alpha7$ plus $\alpha8$, $\alpha9$ plus $\alpha10$, and perhaps other higher order complexes can also form in heterologous expression systems and/or naturally (see reviews cited above and Elgoyhen et al., 2001).

Work in Phoenix toward this project was supported by endowment and capitalization funds from the Men's and Women's Boards of the Barrow Neurological Foundation and Epi-Hab Phoenix, Inc. and by grants 9730 and 9615 from the Arizona Disease Control Research Commission, NS40417 from the National Institutes of Health, and 4366 from the Council for Tobacco Research-USA, Inc.. Studies in Bonn were supported by the Deutsche Forschungsgemeinschraft (Ste769/2-1).

This article is dedicated to the memory of Jian-Hong Peng and Michelle Zhang.

[1] Current address: Department of Neurology, Division of Biology and Biomedical Sciences, Washington University, St. Louis, MO 63110.

ABBREVIATIONS: nAChR, nicotinic acetylcholine receptor(s); $\alpha4\beta2$-nAChR, nicotinic acetylcholine receptor(s) composed of $\alpha4$ and $\beta2$ subunits; h$\alpha4\beta2$-nAChR, human $\alpha4\beta2$-nAChR; HEK, human embryonic kidney; bp, base pair(s); PBS, phosphate-buffered saline; I-EBDN, ^{125}I-labeled iodo-deschloro-epibatidine; RAZ, Ringer's solution supplemented with 0.1 mg/ml of sodium azide; H-EBDN, [^{3}H]epibatidine; DMPP, 1,1-dimethyl-4-phenyl-piperazinium; ACh, acetylcholine; DHβE, dihydro-β-erythroidine; MLA, methyllycaconitine.

Binary complexes of $\alpha 2$, $\alpha 3$, $\alpha 4$, or $\alpha 6$ subunits with $\beta 2$ or $\beta 4$ subunits also can form distinctive nAChR subtypes, at least in heterologous expression systems. $\alpha 5$ and $\beta 3$ subunits seem to be "wild cards" able to integrate into at least some of the α/β binary complexes to form trinary complexes with unique properties, and more than one kind of α or β subunit can exist in some nAChR subtypes (e.g., naturally expressed $\alpha 3\alpha 5\beta 2\beta 4$-nAChR in postganglionic neurons; $\alpha 4\alpha 6\beta 2$-nAChR in heterologous expression systems).

The predominant nAChR subtype in the brain that also displays highest affinity interactions with nicotine contains $\alpha 4$ and $\beta 2$ subunits ($\alpha 4\beta 2$-nAChR; Whiting and Lindstrom, 1987; Flores et al., 1992). $\alpha 4\beta 2$-nAChR have been implicated in perception, cognition, and emotion; in nicotine self-administration, reward, and dependence; and in diseases such as Alzheimer's and epilepsy (Picciotto et al., 1995; Lindstrom, 1996; Lukas, 1998; Cordero-Erausquin et al., 2000; Steinlein, 2001). Consequently, $\alpha 4\beta 2$-nAChR have been widely studied when naturally expressed (e.g., Alkondon and Albuquerque, 1993, 1995; Albuquerque et al., 1998) or when heterologously expressed in the *Xenopus laevis* oocyte system (Elliott et al., 1996; Gopalakrishnan et al., 1996, 1997; Chavez-Noriega et al., 1997; Fenster et al., 1997; Papke et al., 2000). The M10 mouse fibroblast cell line was the first host for stable expression of chick $\alpha 4\beta 2$-nAChR as ligand binding sites (Whiting et al., 1991), but functional responses of $\alpha 4\beta 2$-nAChR in those cells are not robust. HEK cells also have been used for expression of mammalian $\alpha 4\beta 2$-nAChR with good success (Buisson et al., 1996, 2000; Gopalakrishnan et al., 1996, 1997; Cooper et al., 1999; Buisson and Bertrand, 2001). To the first approximation, properties of heterologously and naturally expressed $\alpha 4\beta 2$-nAChR are similar. However, given the importance of $\alpha 4\beta 2$-nAChR, it was reasoned that expression in an alternative model system, the SH-EP1 human epithelial cell line (Ross et al., 1983), was warranted, particularly because SH-EP1 cells may share neuroepithelial origins with neurons; may have a polar nature (basolateral/apical) like neurons (somatodendritic/axonal); perhaps process complex transmembrane proteins as neurons do (Lukas et al., 2002); and could be freely distributed to the academic community. In the process of characterizing human $\alpha 4\beta 2$-nAChR heterologously expressed by human SH-EP1 epithelial cells, interesting and unusual relationships between affinities of nicotinic drugs for radioligand binding and functional sites on $\alpha 4\beta 2$-nAChR have been revealed (see preliminary report by Peng et al., 1999).

Materials and Methods

Cell Culture. Cells of the SH-EP1 human epithelial cell line (kindly provided by Dr. June Biedler, Sloan Kettering Institute for Cancer Research, New York, NY) were grown in Dulbecco's modified Eagle's medium (high glucose, bicarbonate-buffered, with 1 mM sodium pyruvate and 8 mM L-glutamine) supplemented with 10% horse serum, 100 U/ml penicillin, 100 μg/ml streptomycin, and 0.25 μg/ml amphotericin B (all from Invitrogen, Carlsbad, CA) plus 5% fetal bovine serum (Hyclone, Logan, UT) on 100-mm diameter plates in a humidified atmosphere containing 5% CO_2 in air at 37°C (Lukas, 1986; Lukas et al., 1993).

Construction of Human $\alpha 4$ and $\beta 2$ Expression Plasmids and Generation of Stably Transfected Cells and Cell Lines. cDNA encoding a human $\alpha 4$ subunit (Steinlein et al., 1996; see GenBank accession NM_000744 for an update) was excised from the pSPoD vector as a *Hin*dIII-*Sal*I fragment encompassing 54 bp of sequences in the vector polycloning site in the 5′ direction from the 1937 bp of $\alpha 4$ cDNA and 204 bp corresponding to the vector polycloning site and some vector sequences in the 3′ direction from the insert. The ends of the fragment were blunt-ended using Klenow enzyme and ligated into pcDNA3.1/zeo (Invitrogen) cut at the *Eco*RV site to generate the pcDNA3.1/zeo-h$\alpha 4$ construct. cDNA encoding a human $\beta 2$ subunit (Rempel et al., 1998; see GenBank accession NM_000748 for an update) was excised from the pSPoD vector at the *Bgl*II restriction site, blunt-ended, and ligated with pcDNA3.1/hygro (Invitrogen) cut at the *Eco*RV site to generate the pcDNA3.1/hygro-h$\beta 2$ construct. Final constructs were verified by restriction mapping, and full cDNA sequences were confirmed. Some nucleotide differences from the published reference sequences were found, and those producing amino acid residue changes are: $\alpha 4$, tcc(P452S); $\beta 2$, gcg(T26A), ctc(F173L), gcc(V255A), gtg(E449V). These rare polymorphisms have a frequency of less than 1% in the white population. Native nAChR-null SH-EP1 cells (Lukas et al., 1993) were transfected simultaneously with both $\alpha 4$ and $\beta 2$ constructs using electroporation (Gene Pulsar; 960 μF, 0.20 kV/cm, t = 28–36 ms; Bio-Rad, Hercules, CA). Forty-eight hours after transfection, culture medium was supplemented with 0.25 mg/ml zeocin (Invitrogen) and 0.4 mg/ml hygromycin B (130 μg/ml biologically active hygromycin; Calbiochem, San Diego, CA) to begin positive selection for cells expressing dual drug resistance. Growth was monitored until ring cloning was used to isolate single, transfected cell colonies, which were then expanded. Clones were screened for function using $^{86}Rb^+$ efflux assays, and a clone exhibiting high expression of $\alpha 4\beta 2$-nAChR was then subcloned by dilution and repetition of the ring-cloning method. The cell line isolated and used in these studies is called the SH-EP1-pcDNA-h$\alpha 4\beta 2$ line (SH-EP1-h$\alpha 4\beta 2$ cells). These cells were maintained, in medium described above supplemented with zeocin and hygromycin to maintain positive selection of transfectants, as low passage number (1–26 from our frozen stocks) cultures to ensure stable expression of phenotype, and they were passaged once weekly by splitting just-confluent cultures 1/20–1/40 to maintain cells in proliferative growth (Lukas et al., 2002). Reverse transcription-polymerase chain reactions were done initially and regularly thereafter to confirm expression of $\alpha 4$ and $\beta 2$ subunit messages (see Peng et al., 1999; Wu et al., 2001).

Immunofluorescence Cell Labeling. To visualize nAChR $\alpha 4$ and $\beta 2$ subunits on the cell surface, SH-EP1-h$\alpha 4\beta 2$ cells were plated onto 22 × 22-mm glass coverslips and grown for 2 days. Cells were then incubated at 37°C for 30 min in growth medium containing primary monoclonal antibodies generated in Dr. Jon Lindstrom's laboratory against either the nAChR $\alpha 4$ subunit (rat mAb 299; RBI-Sigma, St. Louis, MO) or the nAChR $\beta 2$ subunit (rat mAb 290; RBI-Sigma). Control samples were processed in the absence of primary antibody or used untransfected SH-EP1 cells. After rinsing with phosphate-buffered saline (PBS), cells were fixed with 4% paraformaldehyde for 10 min and rinsed again before blocking for 20 min with PBS containing 4% normal rabbit serum, 1% bovine serum albumin, and 0.4% Triton X-100. Blocking was followed by 30 min incubations with 1% bovine serum albumin-PBS containing biotinylated secondary antibody (rabbit-anti rat IgG; Vector Labs, Burlingame, CA) and then with avidin-Alexa 488 (Molecular Probes, Eugene, OR), with PBS rinses between steps. Staining was visualized using epifluorescence (Olympus IX70; Olympus America, Melville, NY). Transfected SH-EP1 cells heterologously expressing human $\alpha 4\beta 4$-nAChR (Eaton et al., 2000) were used as another negative (for $\beta 2$ subunits) or positive (for $\alpha 4$ subunits) control and showed no staining when probed with anti-$\beta 2$ subunit antibody (data not shown).

^{125}I-Labeled Epibatidine Binding Autoradiography. Cultured cells grown for two days on Lab Tek II CC2 8-well chambered slides (Nalge Nunc International, Naperville, IL) were rinsed in room temperature PBS for 5 min and then incubated in fresh binding buffer (120 mM NaCl, 5 mM KCl, 2.5 mM $CaCl_2$, 50 mM Tris HCl, 1

mM $MgCl_2$, pH adjusted to 7.4 with NaOH) containing 100 pM ^{125}I-labeled iodo-deschloro-epibatidine [(±)-*exo*-2-(2-iodo-5-pyridyl)-7-azabicyclo[2.2.1]heptane; Davila-Garcia et al., 1997; abbreviated here as I-EBDN], alone to define total radioligand binding or in the presence of 100 μM nicotine to define nonspecific binding, for 30 min at 22°C. After radioligand incubation, samples were rinsed twice in 1× binding buffer at 4°C for 10 s each, once in 0.1× buffer at 4°C for 10 s, and then in H_2O at 4°C for 10 s. Subsequently, slides were fixed in 4% paraformaldehyde (50/50 solution, 8% paraformaldehyde, and 0.2 M phosphate buffer, pH 7.2) for 20 min at 22°C before being rinsed briefly in H_2O and air-dried at 22°C. Samples were then subjected to electronic isotope counting using an Instant Imager (PerkinElmer Life Sciences, Boston, MA) to quantify specific (total minus nonspecific) radioligand binding (i.e., integrating counts across defined areas of sections or cultures containing equivalent amounts and densities of cells). After radioligand binding quantification, samples were dipped in NTB-3 nuclear track emulsion (Eastman Kodak, Rochester, NY) and allowed to dry overnight at 22°C in a dust-free environment. Slides were then stored at 4°C for exposure periods ranging from 2 to 5 days (showing a linear grain development response and revealing sites of low-level radioligand binding). After exposure, slides were developed for 3 min at 22°C with Kodak D-19 developer and fixed for 3 min at 22°C with Kodak fixer. Slides were counterstained with 0.5% cresyl violet acetate and serially dehydrated with 50, 75, 85, and 95% ethanol. After ethanol treatments, slides were dipped twice in xylene for 5 min each at 22°C and dry-mounted with Permount. Images were captured using an Olympus IX70 inverted microscope and MagnaFire 2.0 camera and software (Optronics, Goleta, CA) and then stored and maximized for Hi Gauss clarity and sharpness using Image Pro Plus 4.1 (Media Cybernetics, Silver Spring, MD).

Membrane Preparations. Confluent, stably transfected cells were mechanically dislodged using a polypropylene policeman and collected into 50-ml centrifuge tubes (five 100-mm plates per tube). Cells were pelleted and medium removed by low-speed centrifugation, and the cells were then resuspended in 3 ml of ice-cold 5 mM Tris, pH 7.4, to aid in homogenization. Cells were homogenized with a Polytron homogenizer (45 s using a Brinkmann model 10/35 with a PTA10S generator) set at a speed of 70. Homogenized membranes were centrifuged at 45,000*g* for 10 min at 4°C and resuspended in 6 ml of Ringer's solution supplemented with 0.1 mg/ml of sodium azide (RAZ) through two cycles to wash the membranes before final resuspension in ~1 ml of RAZ. Membrane protein was quantified with the bicinchoninic acid protein assay (Pierce, Rockford, IL) according to the manufacturer's instructions. A typical yield for membrane preparations is 0.24 mg of membrane protein per confluent dish. These preparations were stored at 4°C and have a shelf life of at least 1 year for use in ^{3}H-labeled epibatidine (H-EBDN) binding assays.

[^{3}H]EBDN Binding Assays. Membranes prepared as described above were used for H-EBDN (PerkinElmer Life Sciences) binding saturation assays (modified after Houghtling et al., 1994, 1995). Reactions were incubated for 3 to 3.5 h at 25°C in 13 × 100-mm test tubes in a final volume of 6 ml to minimize radioligand depletion. Total radioligand binding was determined for samples that typically contained ~1.5 to 3 μg of membrane protein (~25 and no more than 30 fmol of binding sites, consistent with expression of as much as 12 pmol of nAChR/mg of membrane protein) and H-EBDN to provide a final concentration ranging from 1 pM to 1 nM in RAZ. To determine nonspecific binding, a sister-reaction was carried out at each H-EBDN concentration in the presence of 100 μM nicotine (Sigma Chemical Co., St Louis, MO). Reactions were gently mixed (not vortexed) using an orbital shaker (360-P; Precision Scientific, Winchester, VA) at ~160 rpm. Free H-EBDN was separated from bound H-EBDN using filtration over polyethylenimine-coated, 25-mm diameter GF/C glass fiber discs and a 10-position manifold generating 15 to 20 psi of vacuum. The filter and reaction tubes were then rinsed three times by pumping 8 ml of ice-cold RAZ into the reaction tube and then pouring the rinses over the filter. Filters were air-dried in the manifold by vacuum suction, transferred into liquid scintillation vials, and shaken overnight in 6 ml of Ready-Safe cocktail (Beckman Coulter, Fullerton, CA) before sample H-EBDN was quantified (Tri-Carb 1900 liquid scintillation analyzer; PerkinElmer Life Sciences; 59% efficiency).

For H-EBDN binding competition assays, reactions of 0.8 ml in 1.2-ml microtiter tubes (Life Science Products, Frederick, CO) contained 400 pM H-EBDN. These reactions contained the appropriate volume of RAZ, 100 μl of 3.2 nM H-EBDN, 100 μl of either the appropriate concentration of competing ligand, vehicle, or nicotine to yield a final concentration of 100 μM, and 100 μl of membrane protein (typically 1–3 μg yielding about 25 fmol of binding sites) added in that order, where all ligands and membranes were prepared in RAZ. Reactions were carried out for 2 h at room temperature with shaking. Reactions were terminated by filtration with GF/C filter sheets (soaked in 0.2% polyethylenimine for at least 30 min and rinsed with RAZ just before use) using a 1H-201-A sample processor (Inotech Biosystems, Rockville, MD) in the 96-well cutting head configuration. Samples aspirated onto the GF/C sheets were rinsed three times using ice-cold RAZ. Filters were transferred to PET 96-well plates (PerkinElmer Wallac, Gaithersburg, MD), and 200 μl of Ready-Safe cocktail was added before incubation for at least 12 h and quantification of bound radioligand by scintillation counting (38% efficiency; PerkinElmer Wallac Microbeta Trilux 1450).

H-EBDN binding association studies were carried out using 0.6-ml reaction volumes containing H-EBDN at final concentrations of 100, 333, 667, and 1000 pM and 100 μl of membranes (typically 1–2 μg of protein and ~15 fmol of binding sites). Reaction times varied between 0 and 75 min, and samples were processed as for radioligand competition studies. H-EBDN dissociation studies involved reactions at 1 nM as for association studies but carried out for 2 h before nicotine was added to a final concentration of 100 μM to initiate dissociation. Control samples not supplemented with nicotine or supplemented with nicotine throughout were used to check for degradation of binding sites during the course of the assay. This chemical dilution protocol to study kinetics of H-EBDN dissociation was used instead of a physical dilution design because it seemed that H-EBDN and/or its binding sites degraded during the necessarily long times at high dilution required for physical dilution studies (data not shown).

$^{86}Rb^+$ Efflux Assays. Cells were harvested at confluence from 100-mm plates by mild trypsinization (Irvine Scientific, Santa Ana, CA) before being resuspended in complete medium and evenly seeded at a density of one confluent 100-mm plate per 24-well plate (Falcon Plastics, Oxnard, CA; ~100–125 μg of total cell protein per well in a 500 μl volume). After cells had adhered (generally overnight, but no sooner than 4 h later), medium was removed and replaced with 250 μl per well of complete medium supplemented with ~300,000 cpm of $^{86}Rb^+$ (PerkinElmer Life Sciences; counted at 40% efficiency using Cerenkov counting and the PerkinElmer Tri-Carb 1900 liquid scintillation analyzer). After at least 4 h and typically overnight, $^{86}Rb^+$ efflux was measured using the "flip-plate" technique (Lukas et al., 2002). Briefly, after aspiration of the bulk of $^{86}Rb^+$ loading medium from each well of the "cell plate", each well containing cells was rinsed three times with 2 ml of fresh $^{86}Rb^+$ efflux buffer (130 mM NaCl, 5.4 mM KCl, 2 mM $CaCl_2$, 5 mM glucose, and 50 mM HEPES, pH 7.4) to remove extracellular $^{86}Rb^+$. After removal of residual rinse buffer by aspiration, the flip-plate technique was used again to simultaneously introduce fresh efflux buffer containing drugs of choice at indicated final concentrations from a 24-well "efflux/drug plate" into the wells of the cell plate. After a 3-min incubation, the solution was "flipped" back into the efflux/drug plate, any remaining medium was removed by aspiration, and the cells in the cell plate were lysed and suspended by addition of 2 ml of 0.1 M NaOH, 0.1% SDS to each well. Suspensions in each well were then subjected to Cerenkov counting (PerkinElmer Wallac Micobeta Trilux 1450; 25% efficiency) after placement of inserts (PerkinElmerWallac 1450-109) into each well to minimize cross-talk

between wells. For each experiment, normalization and quality control measurements were made of total $^{86}Rb^+$ efflux in samples containing a fully efficacious dose of 1 mM carbamylcholine and of nonspecific $^{86}Rb^+$ efflux measured using either samples containing 1 mM carbamylcholine plus 100 μM mecamylamine, which gave full block of agonist-induced or spontaneous, nAChR-mediated ion flux, or samples containing efflux buffer alone to assess any contributions caused by spontaneous nAChR-mediated ion flux. Intrinsic agonist activity of test drugs was ascertained in samples containing that drug only at different concentrations and was normalized, after subtraction of nonspecific efflux, to specific efflux assessed using carbamylcholine and efflux-buffer-only controls. Antagonist activity was determined for test drugs at different concentrations in the presence of 1 mM carbamylcholine and was normalized, after subtraction of nonspecific efflux, to specific efflux ascertained using carbamylcholine and efflux buffer-only controls. $^{86}Rb^+$ in both cell plates and efflux/drug plates was periodically determined to ensure material balance (i.e., that the sum of $^{86}Rb^+$ released into the efflux/drug plate and $^{86}Rb^+$ remaining in the cell plate were the same for each well) and to determine efficiency of $^{86}Rb^+$ loading (the percentage of applied $^{86}Rb^+$ actually loaded into cells). Specific $^{86}Rb^+$ efflux was determined in absolute terms and as a percentage of loaded $^{86}Rb^+$. Depending on cell density and the concentration of $^{86}Rb^+$ in the loading medium, SH-EP1-h$\alpha4\beta2$ cells typically display specific efflux of 5,000 to 15,000 cpm of $^{86}Rb^+$ per sample with a ratio of total to nonspecific efflux of 10:1, and total efflux is about half of loaded $^{86}Rb^+$.

Data Analysis. Parameters [dissociation constant K_D and maximum binding level B_{max}; $B = B_{max}/(1 + (K_D/X)^{nH})$] for specific radioligand binding were determined from nonlinear graphic analysis (Prism; GraphPad Software, San Diego, CA) of plots of specific binding, B, as a function of the free concentration of radioligand, X, and for Hill coefficient, n_H, for each sample, where specific binding was defined as total minus nonspecific binding, and nonspecific binding was calculated from linear regression analysis of H-EBDN binding in the presence of 100 μM nicotine. A Scatchard analysis was also done for illustrative purposes, but not to determine specific binding parameters. Initial radioligand binding competition studies were done under conditions of ligand depletion (in the presence of 100 pM H-EBDN); i.e., samples were used in which greater than 10% of the radioligand was bound, meaning that free radioligand concentrations could not be assumed to be equal at equilibrium to their initial values or equal across samples and that nonspecific binding could not be assumed to be the same for samples with the same total concentration of radioligand. Iterative nonlinear regression fits to the data using equations for homologous or heterologous competition binding with radioligand depletion (Prism) gave reasonably consistent measures of IC_{50} and K_i values for most, but not all, ligands. Therefore, data presented derive only from studies done to eliminate ligand depletion (i.e., at an initial H-EBDN concentration of 400 pM). Specific binding, B, as a function of competing drug concentration, X, was plotted and fit to the Hill equation, $B = B_{max} / (1 + (X/IC_{50})^{nH})$ for competing drug concentration to give half-maximal inhibition of radioligand binding, IC_{50}, control specific binding B_{max}, and the Hill slope, n_H (Prism). Radioligand association studies were analyzed by iterative nonlinear regression using the equation for a monophasic exponential process $Y = Y_{max}(1 - e^{-kt})$, for association constant, k (k_{on} or k_1), and maximal binding, Y_{max} (Prism). Radioligand dissociation studies were analyzed by iterative nonlinear regression using the equation for a monophasic exponential process $Y = Y_{max}(e^{-kt})$, for dissociation constant, k (k_{off} or k_{-1}), and maximal binding, Y_{max}, where the asymptotic approach at long t was set to zero (Prism). Ion flux assays also were fit to the Hill equation, but they made measures of specific ion flux, F, as a percentage of control, F_{max}, and determined EC_{50} ($n > 0$ for agonists) or IC_{50} ($n < 0$ for antagonists) values (Prism). In some cases, biphasic dose-ion flux response curves were evident and were fit to a two-phase Hill equation from which EC_{50} and Hill coefficients for the rising, agonist phase and IC_{50} and Hill coefficients for the falling, self-inhibitory phase could be determined (Prism). Most ion flux data were fit allowing maximum and minimum ion flux values to be determined by curve fitting, but in some cases in which antagonists or agonists had weak functional potency, minimum ion flux was set at 0% of control or maximum ion flux was set at 100% of control, respectively.

Materials. All other techniques and commercial sources for reagents were as indicated earlier (Lukas, 1986; Bencherif and Lukas, 1993; Peng et al., 1999).

Results

SH-EP1-h$\alpha4\beta2$ cells, positive for human $\alpha4$ and $\beta2$ subunit message and isolated based on their expression of functional h$\alpha4\beta2$-nAChR, were subjected to H-EBDN binding saturation assays under conditions that eliminated or minimized confounding effects of ligand depletion that can occur with such a high-affinity radioligand. The results of a typical binding saturation profile are shown in Fig. 1, and results from three independent studies yielded an average macroscopic K_D value (value shown on Fig. 1) of 10.1 ± 1.4 pM, consistent with the presence of a single class of noninteracting binding sites. B_{max} values derived from these studies using 1 to 9 μg of membrane protein per assay were 14.4 ± 0.3 fmol/assay, yielding a concentration of h$\alpha4\beta2$-nAChR H-EBDN binding sites of between 1,600 and 14,000 fmol/mg. Although not studied systematically, variation in B_{max} values reflected differences in cell passage (sometimes higher passage leads to loss of nAChR expression) and/or cell plating density at the time of harvest for assay (highest expression

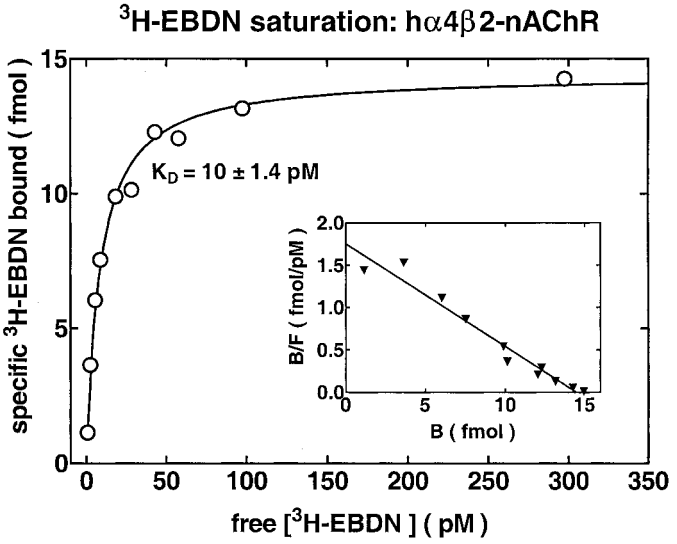

Fig. 1. Saturation analysis for [^{3}H]EBDN binding to a SH-EP1-h$\alpha4\beta2$ cell membrane preparation. Reaction mixtures containing ~1 to 5 μg of membrane protein from SH-EP1-pcDNA-h$\alpha4\beta2$ cells and [^{3}H]EBDN at the indicated final concentrations (abscissa; free radioligand; picomolar) were processed for 3 h to determine specific [^{3}H]EBDN binding (○; ordinate; femtomoles). Nonspecific binding determined using samples containing 100 μM nicotine was defined by the equation [(350[[^{3}H]EBDN] (nanomolar)) + 6] fmol/mg and was ~14% of total binding at 100 pM [^{3}H]EBDN. Results from the illustrated study yielded a K_D value (± S.E.M.) of 8.39 ± 0.76 pM and a B_{max} value (± S.E.M.) of 14.4 ± 0.3 fmol for this preparation ($r^2 = 0.99$). B_{max} values determined from independent repeated saturation binding assays using other preparations were 4.8 ± 0.3 pmol/mg of membrane protein for a mean (± S.E.M.) K_D value of 10.1 ± 1.4 pM. Inset, Scatchard plot of bound/free [^{3}H]EBDN (▼; ordinate; femtomoles/picomolar) versus bound [^{3}H]EBDN (abscissa; femtomoles).

occurs for cells near confluence). These results showed that heterologously expressed h$\alpha4\beta2$-nAChR engage in very high-affinity, specific binding of H-EBDN.

Association rate kinetics studies showed that H-EBDN binding to h$\alpha4\beta2$-nAChR in SH-EP1-h$\alpha4\beta2$ cells occurs as a single phase of interaction (Fig. 2). Observed rates of H-EBDN binding varied between 0.13 and 0.78 min^{-1} (half-times of 0.89–5.3 min) with H-EBDN concentration between 0.1 and 1 nM. A plot (Fig. 2, inset) of observed association rates versus H-EBDN concentration yielded a slope corresponding to k_1 of 0.74 ± 0.02 min^{-1} nM^{-1} and a y-intercept corresponding to k_{-1} of 0.046 ± 0.012 min^{-1}, yielding a microscopic K_D of 62 pM, substantially higher than the measured macroscopic K_D. Because of concern that the estimate of k_{-1} from these studies might be misleading, independent empirical studies of dissociation kinetics were done. These revealed a slower apparent dissociation rate of 0.013 ± 0.001 min^{-1} (half-time of ~53 min; simple monophasic decay indicative of a single class of noninteracting sites), yielding a microscopic K_D of 18 pM (Fig. 3), in better agreement with the macroscopic K_D determination.

To assess the uniformity of expression of nAChR subunit protein across cells, and as a guide for electrophysiological studies (see Wu et al., 2001, for preliminary descriptions of findings to be described in detail elsewhere), immunofluorescence analysis of nAChR $\alpha4$ and $\beta2$ subunit expression was done. There was no staining of control, untransfected SH-EP1 cells using either antibody, and there was no staining of a cell line expressing human $\alpha4$ and $\beta4$ subunits with the anti-$\beta2$ subunit antibody (negative control results not shown). However, cell surface immunostaining of SH-EP1-h$\alpha4\beta2$ cells with either $\alpha4$ or $\beta2$ subunits was positive and revealed comparable patterns of antigen distribution, with virtually every cell showing some evidence of surface expression (Fig. 4). In many cases, staining was bright and punctate, suggesting clustering of h$\alpha4\beta2$-nAChR. Staining also was evident in processes emanating from cell bodies, often at the tips of such processes, and puncta from adjacent cells were sometimes in close apposition.

As another approach to ascertain the uniformity of expression of h$\alpha4\beta2$-nAChR across cells, and also to guide electrophysiological studies, I-EBDN-receptor binding autoradiography was executed (Fig. 5). Studies using SH-EP1-h$\alpha4\beta2$ cells treated with I-EBDN in the presence of excess nicotine to define nonspecific binding and cell labeling showed minimal silver halide grain development over cell bodies and very low overall silver halide grain development defined as background. By contrast, cells treated without nicotine and incubated only in I-EBDN to define total binding exhibited dense silver halide grain development over cell bodies, especially over populations of cells that were tightly packed together. Silver grain development over individual cells could be distinguished within intercellular boundaries (i.e., where cells were in close proximity) and on solitary cells. More than 80% of cells showed some labeling, and about 35% of cells were heavily labeled.

Radioligand binding competition studies done under conditions to eliminate, minimize, or account for ligand depletion indicated that unlabeled epibatidine is the most potent of the drugs used to inhibit specific H-EBDN binding to h$\alpha4\beta2$-nAChR in transfected SH-EP1 cell membrane preparations (Fig. 6; Table 1). All nicotinic agonists were able to fully block H-EBDN binding, having rank order binding inhibition potency and IC_{50} values of: 490 pM epibatidine (EBDN) ≫ 10 nM cytisine > 81 nM nicotine ≫ 740 nM acetylcholine (ACh) ~ 830 nM 1,1-dimethyl-4-phenyl-pipera-

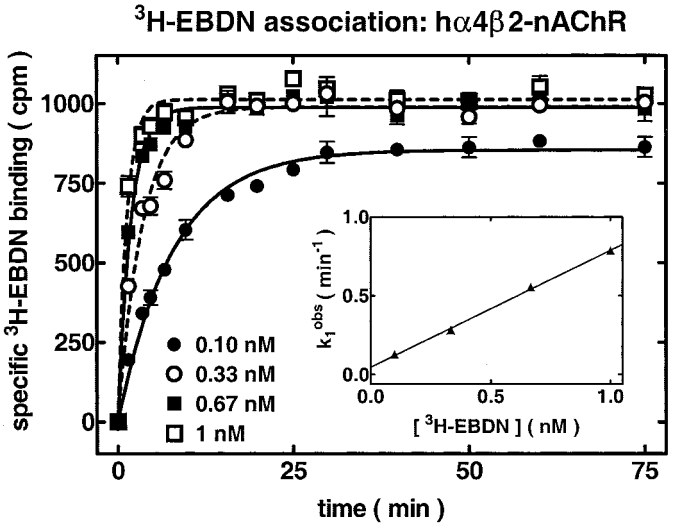

Fig. 2. [^{3}H]EBDN association rate studies. Reaction mixtures containing SH-EP1-h$\alpha4\beta2$ cell membrane preparations (typically containing ~3 μg of protein) and 0.1 (●), 0.33 (○), 0.67 (■), or 1 nM (□) [^{3}H]EBDN were incubated for the indicated times (abscissa; minutes) before being processed for determination of specific [^{3}H]EBDN binding (ordinate; counts per minute). Lines drawn through the data points are best fit curves (r^2 = 0.97 to 0.98 for all curves; data points are averages from three independent studies) yielding k_1^{obs} values of 0.13 ± 0.01 at 0.1 nM, 0.28 ± 0.01 at 0.33 nM, 0.56 ± 0.08 at 0.67 nM, and 0.78 ± 0.06 at 1 nM [^{3}H]EBDN and half-times for association ranging between 5.3 and 0.89 min at 0.1 and 1 nM [^{3}H]EBDN, respectively. Inset: plots of k_1^{obs} (ordinate; per minute) as a function of [[^{3}H]EBDN] (abscissa; nanomolar) have a slope (k_1 value) of 0.74 ± 0.02 min^{-1} nM^{-1} and a y-intercept (k_{-1} value) of 0.046 ± 0.012 min^{-1}.

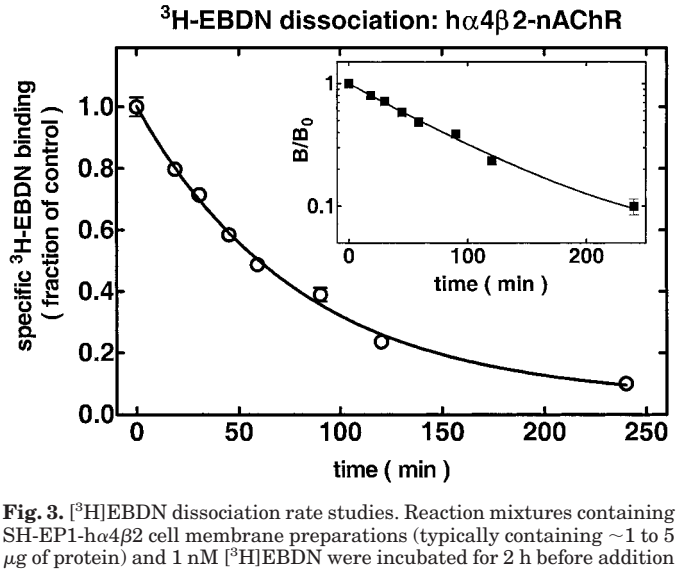

Fig. 3. [^{3}H]EBDN dissociation rate studies. Reaction mixtures containing SH-EP1-h$\alpha4\beta2$ cell membrane preparations (typically containing ~1 to 5 μg of protein) and 1 nM [^{3}H]EBDN were incubated for 2 h before addition to a final concentration of 100 μM nicotine at "time 0" before separation of free from bound [^{3}H]EBDN at the indicated times (abscissa; minutes) to allow determination of specific [^{3}H]EBDN binding (○; ordinate; fraction of control; data points are averages from three independent studies). The line drawn through the data points is the best fit curve yielding an apparent rate constant for dissociation of 0.013 ± 0.001 min^{-1}. Inset, same data as in the main graph but plotted on the y-axis as B/B_0 on a log scale.

zinium (DMPP) ≫ 6.0 μM carbamylcholine ≥7.1 μM acetylthiocholine ≫ 290 μM choline. Lobeline (IC_{50} = 76 nM) had ligand binding competition potency greater than any antagonist and like that of nicotine, and suberyldicholine (IC_{50} = 520 nM) had ligand binding competition potency like that of acetylcholine (Fig. 6, Table 1). Of the antagonists tested, only dihydro-β-erythroidine (DHβE) gave high affinity, full (over the concentration ranges actually studied) blockade of H-EBDN binding (IC_{50} = 3.5 μM; Fig. 6, Table 1). Rank order binding inhibition potency and IC_{50} values for the other antagonists were: 52 μM decamethonium ≥ 81 μM *d*-tubocurarine ~ 95 μM methyllycaconitine (MLA) ≥ 120 μM succinylcholine > 760 μM alcuronium ~ 980 μM vecuronium > 1.9 mM hexamethonium ~ 2.3 mM pancuronium >> 1 mM eserine (Fig. 6, Table 1). Mecamylamine (data not shown) exhibited no inhibition at all up to 100 μM.

Function of hα4β2-nAChR expressed in transfected SH-EP1 cells was assessed using $^{86}Rb^{+}$ efflux assays (electrophysiological characterization of hα4β2-nAChR will be reported in a different series of communications; e.g., see Wu et al., 2001). Agonist log dose-response profiles show simple, sigmoid shapes and full functional efficacy for EBDN, ACh, and carbamylcholine; bell shapes for nicotine (~full efficacy) and suberyldicholine (low efficacy); sigmoid shapes but submaximal efficacy for cytisine, DMPP, and perhaps acetylthiocholine; and very weak potency for choline (Fig. 7, Table 2).

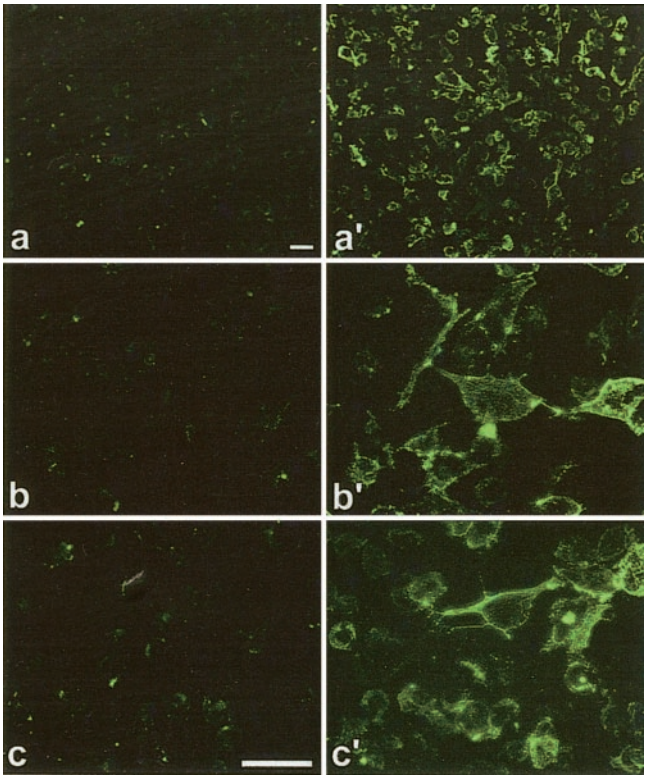

Fig. 4. Immunofluorescence staining of α4 and β2 subunits. SH-EP1-hα4β2 cells were probed using primary monoclonal antibodies against either α4 (a′, b′) or β2 (c′) subunits, biotinylated secondary antibody, and avidin-Alexa 488 or in the absence of primary antibody (a, b, c) as described under *Materials and Methods*. Epifluorescence images were taken at 200× (a, a′) or 600× (b, b′, c, c′) magnification (calibration bars for each magnification set are 50 μm).

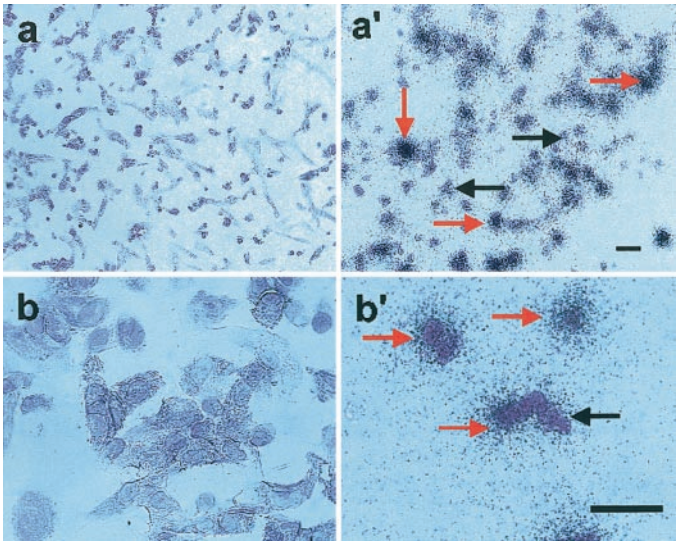

Fig. 5. I-EBDN-receptor binding autoradiography. SH-EP1-hα4β2 cells were treated with I-EBDN in the presence of 10 mM nicotine to define nonspecific binding (left; a, b) or with I-EBDN alone to define total binding (right; a′, b′). Red arrows on the right indicate areas of specific I-EBDN binding, and black arrows indicate unlabeled cells. The higher level of diffuse staining seen in a′ and b′ as well as the intense staining over cell bodies in these images are both hallmarks of specific I-EBDN binding. Images were taken at 200× (a, b) or 400× (a′, b′) magnification (calibration bars for each image are 50 μm)

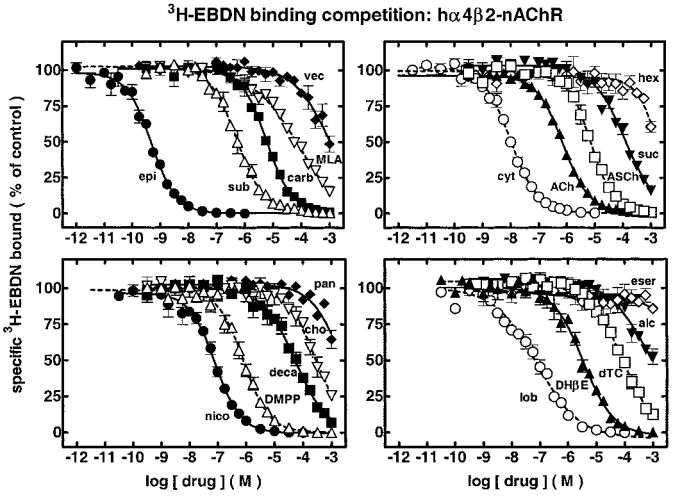

Fig. 6. Ligand competition profiles for blockade of specific [^{3}H]EBDN binding to sites on SH-EP1-hα4β2 cells. Reaction mixtures containing SH-EP1-hα4β2 cell membrane preparations (typically containing ~1 to 5 μg of protein), 400 pM [^{3}H]EBDN, and the indicated drugs were used to assess the concentration dependence (abscissa; molar, log scale) for competition toward specific [^{3}H]EBDN binding (ordinate; percentage of control). Results are the averages of at least three separate experiments. Competition profiles for: top left, Epibatidine (epi; ●), suberyldicholine (sub; △), carbamylcholine (carb; ■), MLA (▽) and vecuronium (vec; ♦); top right, cytisine (cyt; ○), ACh (▲), acetylthiocholine (ASCh; □), succinylcholine (suc; ▼) and hexamethonium (hex; ◇); bottom left, nicotine (nico; ●), DMPP (△), decamethonium (deca; ■), choline (cho; ▽) and pancuronium (pan; ♦); and bottom right, lobeline (lob; ○), DHβE (▲), *d*-tubocurarine (dTC; □), alcuronium (alc; ▼) and eserine (eser; ◇). Log IC_{50} values and Hill coefficients (± S.E.M.) are provided in Table 1, and IC_{50} or K_i values are indicated in the text or in Table 3. Maximum and minimum values for specific [^{3}H]EBDN binding obtained from curve fitting were 100 ± 5% or 0 ± 5%, respectively, of control specific binding except for methyllycaconitine (minimum of −11 ± 10% of control) and alcuronium (maximum of 107 ± 2% of control), and except for fits to the Hill equation for pancuronium, vecuronium, alcuronium, decamethonium, succinylcholine, eserine, choline, and hexamethonium, which were based on minimum binding values fixed at 0% of control specific binding. Mecamylamine showed no inhibition at all up to a concentration of 100 μM.

Lobeline (not shown) and succinylcholine had negligible efficacy. Rank order agonist potency and EC_{50} values (maximum efficacy in parentheses) were: 8.5 nM epibatidine (100%) $\gg$ 850 nM nicotine (104%) $>$ 1.3 μM cytisine (40%) $\sim$ 1.3 μM suberyldicholine (13%) $\sim$ 1.7 μM ACh (104%) $\sim$ 1.9 μM DMPP (80%) $>$ 17 μM carbamylcholine (97%) $>$ 100 μM acetylthiocholine (75%) $\gg$ 3.8 mM (estimated) choline (22% at 1 mM). Self-inhibitory IC_{50} values were also determined for nicotine (5.8 mM) and suberyldicholine (200 μM; Table 2).

Antagonist log dose-response profiles showed full inhibition of h$\alpha4\beta2$-nAChR function stimulated by 1 mM carbamylcholine (Fig. 8; Table 2). Rank order antagonist potency and IC_{50} values (Fig. 8; Table 2) were: 470 nM mecamylamine $>$ 1.5 μM DHβE $>$ 6.6 μM MLA $>$ 11 μM hexamethonium $>$ 21 μM lobeline $\geq$ 26 μM alcuronium $\sim$ 28 μM vecuronium $>$ 62 μM *d*-tubocurarine $>$ 91 μM pancuronium $>$ 130 μM eserine $\geq$ 300 μM decamethonium $>$ 360 μM suberyldicholine. Succinyldicholine and α-bungarotoxin had negligible antagonist activity out to 1 mM and 1 μM, respectively.

When agonist dose-response studies were done alone or in the presence of antagonists at concentrations near their IC_{50} values (Fig. 9), profiles obtained revealed that block by DHβE, MLA, or decamethonium was surmountable by increasing agonist concentrations, suggesting a competitive mechanism of inhibition of function. By contrast, block by mecamylamine or eserine was not surmountable at higher agonist concentrations (Fig. 9), suggestive of a noncompetitive mechanism of action. EC_{50} values for carbamylcholine in the presence of pancuronium, hexamethonium, or *d*-tubocurarine were higher than in the absence of antagonists, but surmountability of block was not clearly evident, suggesting a mixture of competitive and noncompetitive block (Fig. 9). These suggestions were corroborative with indications from radioligand binding competition assays (see Table 3). For example, those antagonists suggested by functional assays to be noncompetitive inhibitors inhibited H-EBDN binding not at all or at concentrations much higher than those needed to inhibit function. By contrast, those antagonists exhibiting competitive mechanisms of functional block inhibited binding of H-EBDN at concentrations more consistent with their functional IC_{50} values.

To lend insight into relationships between h$\alpha4\beta2$-nAChR ligand binding and functional effects, functional EC_{50} or IC_{50} values from $^{86}Rb^+$ ion flux assays and H-EBDN binding competition binding K_i values were compared (Table 3). The latter values were derived from binding competition IC_{50} values using the Cheng-Prusoff correction ($K_i = IC_{50}/[1+(400/10)]$ for an H-EBDN K_D for interaction at h$\alpha4\beta2$-nAChR of 10 pM and a concentration of H-EBDN used in the radioligand binding competition assays of 400 pM). The Cheng-Prusoff correction for EBDN competition toward H-EBDN binding gives a K_i value of 12 pM, in reasonably good agreement with the saturation binding K_D value of 10 pM. In principle, the Cheng-Prusoff correction also could be applied to functional IC_{50} values (obtained using 1 mM carbamylcholine, which has a functional EC_{50} value of 17 μM). However, because this correction theoretically would apply only to competitive antagonists, and mechanisms of action were not established for all of the antagonists studied, the correction was not applied. Nevertheless, the ratio *F/B* of functional EC_{50} or IC_{50} to the binding competition K_i was calculated and is presented in the last column of Table 3 to guide interpretation and discussion of the results. Of the agonists examined, only cytisine has a ligand binding competition IC_{50} value that is out of rank with agonist functional EC_{50} values, yielding a high functional/binding affinity ratio (F/B = 5300; Table 3). The other agonists fall into two classes, those with F/B ratios of $\sim$100 (suberyldicholine, ACh, DMPP, carbamylcholine), indicating that their affinity for the H-EBDN-binding state is $\sim$100-fold higher than their affinity for the basal, nonfunctional state of h$\alpha4\beta2$-nAChR, and those with F/B ratios of $\sim$400 to 700 (EBDN, nicotine, acetylthiocholine, choline) displaying even higher relative affinity for the H-EBDN-binding state. Interestingly, lobeline is the only antagonist that has a comparatively high F/B ratio (11000),

TABLE 1

Parameters for drug competition toward specific [^{3}H]EBDN binding to hα 4β2-nAChR in transfected SH-EP1 cells

Radioligand binding competition assays were conducted as described under *Materials and Methods* and in the legend to Fig. 6. Results were fit to the logistic equation to determine log IC_{50} values ($\pm$ S.E.M.), mean IC_{50} values, and Hill coefficients ($\pm$ S.E.M.).

Drug	log IC_{50}	IC_{50}	n_H
		μM	
Epibatidine	-9.31 ± 0.04	0.00049	-0.98 ± 0.08
Cytisine	-8.00 ± 0.03	0.010	-0.89 ± 0.05
Lobeline	-7.12 ± 0.07	0.076	-0.58 ± 0.05
Nicotine	-7.09 ± 0.05	0.081	-0.96 ± 0.09
Suberyldicholine	-6.28 ± 0.03	0.52	-0.91 ± 0.05
ACh	-6.13 ± 0.02	0.74	-0.92 ± 0.03
DMPP	-6.08 ± 0.05	0.83	-0.97 ± 0.09
DHβE	-5.46 ± 0.06	3.5	-0.81 ± 0.07
Carbamylcholine	-5.22 ± 0.03	6.0	-0.97 ± 0.06
Acetylthiocholine	-5.15 ± 0.03	7.1	-1.06 ± 0.08
Decamethonium	-4.28 ± 0.04	52	-0.77 ± 0.05
d-Tubocurarine	-4.09 ± 0.09	81	-0.73 ± 0.06
MLA	-4.02 ± 0.03	95	-0.57 ± 0.03
Succinylcholine	-3.92 ± 0.04	120	-0.76 ± 0.06
Choline	-3.54 ± 0.04	290	-0.84 ± 0.07
Alcuronium	-3.12 ± 0.11	760	-0.59 ± 0.11
Vecuronium	-3.01 ± 0.06	980	-0.69 ± 0.08
Hexamethonium	-2.73 ± 0.15	1,900	-1.13 ± 0.34
Pancuronium	-2.63 ± 0.11	2,300	-0.82 ± 0.14
Mecamylamine	$\ll -4$	$\gg 100$	
Eserine	< -3	$>1{,}000$	

suggesting that it has ~4 orders of magnitude higher affinity for the H-EBDN-binding state than for the functional, basal state. Of the other antagonists, succinylcholine and decamethonium have agonist-like F/B ratios, suggesting higher affinity interaction with the H-EBDN-binding state than expected based on their functional inhibitory potencies. F/B ratios are between 1 and 2 for classic curarimimetics such as pancuronium, vecuronium, and alcuronium, suggesting close correspondence between their binding affinities for sites involved in functional agonist and H-EBDN binding. By contrast, the F/B ratio for mecamylamine is <0.02, consistent with its demonstrated noncompetitive mechanism of hα4β2-nAChR functional block. However, F/B rations range between 31 for *d*-tubocurarine and 0.24 for hexamethonium, agents with mixed competitive/noncompetitive actions, and between 230 and 2.8 for competitive antagonists decamethonium and MLA (with DHβE having an intermediate F/B ratio). Thus, the broad distribution of F/B ratios across and within classes of agonists, competitive antagonists, and noncompetitive/mixed antagonists indicates that this simplified method of analysis may not adequately describe hα4β2-nAChR-ligand interactions.

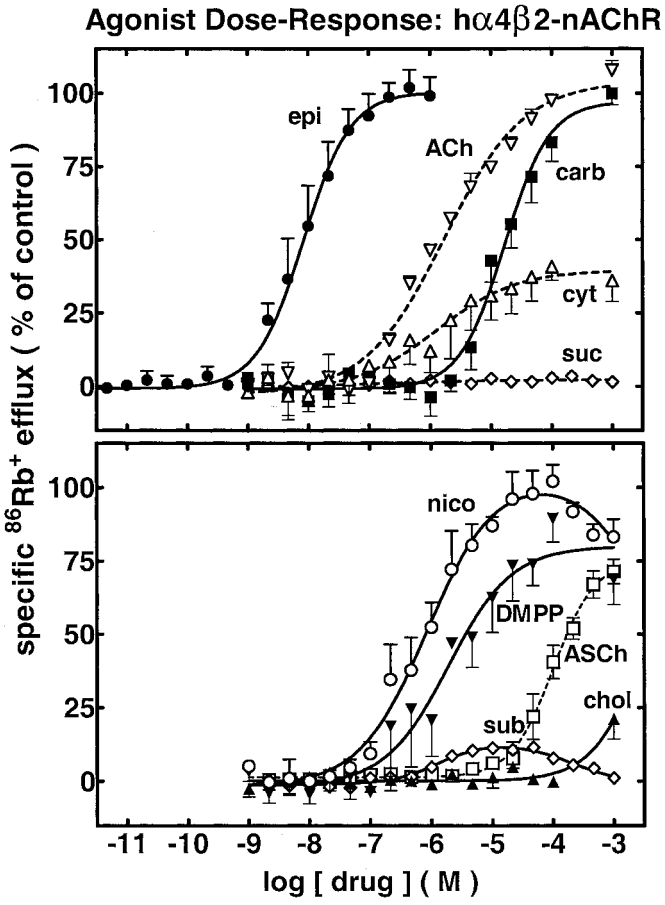

Fig. 7. Agonist dose-response profiles for stimulation of hα4β2-nAChR function. Specific $^{86}Rb^+$ efflux (ordinate; percentage of control) was determined as described under *Materials and Methods* in the presence of the indicated concentrations (abscissa; log molar scale) of: top, Epibatidine (epi; ●), ACh (▽), carbachol (carb; ■), cytisine (cyt; △), or succinylcholine (◇); bottom, nicotine (nico; ○), DMPP (▼), suberyldicholine (sub; ◇), acetylthiocholine (ASCh; □), or choline (chol; ▲). Log EC_{50} values and Hill coefficients (± S.E.M.) are provided in Table 2, and EC_{50} values are indicated in the text and in Table 3. Self-inhibitory IC_{50} values are indicated in parentheses in Table 3, and corresponding log IC_{50} values and Hill coefficients are indicated in Table 2.

Discussion

The major findings of this study are that human α4β2-nAChR can be stably transfected into native nAChR-null SH-EP1 human epithelial cells, express high affinity for the radioligand H-EBDN, exhibit generally higher binding affinity for agonists than for antagonists, and display functional properties notable for high-affinity agonism by EBDN and nicotine and high-affinity antagonism by mecamylamine and DHβE.

The success reported here in generating a stably transfected SH-EP1 cell line heterologously expressing hα4β2-nAChR provides a model system for studies of α4β2-nAChR other than the lines developed using HEK cells and under restricted availability from labs in the private sector (Buisson et al., 1996, 2000; Gopalakrishnan et al., 1996, 1997; Buisson and Bertrand, 2001). Excellent expression of functional α4β2-nAChR assayable using ion flux (current study; Ferchmin et al., 2001), electrophysiological (see Wu et al., 2001), or calcium imaging techniques (Pacheco et al., 2001) has been achieved, giving advantage over transfected cell lines expressing rat α4β2-nAChR–like binding sites but not yet shown to express high levels of functional receptors (Cooper et al., 1999; Shafaee et al., 1999). The expression of hα4β2-nAChR from entirely wild-type subunits and for cells maintained using conventional techniques has advantages over other model systems that have employed altered incubation temperatures or have resorted to creation of chimeric subunits with transmembrane and cytoplasmic domains from non-nAChR subunits to get good surface and functional expression (Cooper et al., 1999). Immunofluorescence and receptor binding autoradiographic analyses indicate that virtually all cells from the isolated clone make both α4 and β2 subunit proteins and binding sites. These analyses suggest that ligand binding site activity and subunit gene transcription is relatively stable and at least evident through the cell cycle. These analyses, ligand binding studies, and functional assessments also indicate that expression of hα4β2-nAChR is relatively stable and at least evident through cell passage.

H-EBDN binding profiles for hα4β2-nAChR expressed in transfected SH-EP1 cells match in many ways those for other preparations heterologously or naturally expressing human/mammalian α4β2-nAChR (Lukas, 1990; Houghtling et al., 1994, 1995; Gopalakrishnan et al., 1996). IC_{50} values are difficult to compare for experiments done using different radioprobes and conditions, and K_i values do not always match precisely across experiments, perhaps because of species differences in the α4β2-nAChR being assayed. Nevertheless, the rank order for competing ligands is very similar across these studies. Moreover, these studies all show a striking imbalance between agonist and antagonist affinities for α4β2-nAChR binding sites, whether they be identified using radiolabeled EBDN, nicotine, ACh, methylcarbamylcholine, or cytisine (Romano and Goldstein, 1980; Marks and Collins, 1982; Schwartz et al., 1982; Abood and Grassi, 1986; Lukas, 1990; Pabreza et al., 1991; Houghtling et al., 1994, 1995; Gopalakrishnan et al., 1996). There is a clear lack of inhibition of radioagonist binding by mecamylamine or hexamethonium, but this can be rationalized based on their actions as

functional noncompetitive antagonists that must have higher affinity interactions at sites distinct from the agonist binding domain. In absolute terms, K_i values for blockade of radioligand binding to heterologously expressed h$\alpha4\beta2$-nAChR in SH-EP1 cells (this study; competition toward H-EBDN binding) or in HEK cells (Gopalakrishnan et al., 1996; competition toward [^{3}H]cytisine binding) are within a factor of 2 except for EBDN (12 pM in this study but 70 pM in Gopalakrishnan et al., 1996). This could reflect influences of ligand depletion in the latter study, because extremely high-affinity binding of EBDN or other nicotinic agonists to h$\alpha4\beta2$-nAChR when heterologously expressed at high levels means that caution need be applied in conduct and interpretation of radioligand binding assays. It also means that ligand depletion in functional studies could occur at low agonist doses, but in practice this is not an evident problem because of the lower affinity functional EC_{50} vales for agonists compared with radioligand binding K_i or even IC_{50} values.

TABLE 2

Parameters for agonist and/or antagonist action at hα 4β 2-nAChR.

$^{86}Rb^+$ efflux assays were conducted as described under *Materials and Methods* and in the legends to Figs. 7 and 8. Results were fit to the logistic equation to determine log EC_{50} values (for agonists) or IC_{50} values (for antagonists) and Hill coefficients (presented ± S.E.M.). Functional log IC_{50} values and Hill numbers given in parentheses for nicotine and suberyldicholine are from fits to the self-inhibitory phase of agonist dose-response profiles for those drugs.

Drug	log EC_{50}	n_H	log IC_{50}	n_H
Epibatidine	−8.07 ± 0.08	1.12 ± 0.22		
Nicotine	−6.07 ± 0.21	0.79 ± 0.21	(−2.24 ± 0.93)	(−0.76 ± 1.15)
Cytisine	−5.90 ± 0.32	0.67 ± 0.31		
Suberyldicholine	−5.89 ± 0.19	1.15 ± 0.39	(−3.69 ± 0.23)	(−0.95 ± 0.35)
			−3.44 ± 0.34	−0.91 ± 0.28
ACh	−5.77 ± 0.08	0.67 ± 0.07		
DMPP	−5.72 ± 0.19	0.84 ± 0.26		
Carbamylcholine	−4.78 ± 0.07	1.18 ± 0.19		
Acetylthiocholine	−4.00 ± 0.06	1.25 ± 0.16		
Choline	<-3			
Mecamylamine			−6.33 ± 0.05	−1.17 ± 0.15
DHβE			−5.82 ± 0.05	−1.36 ± 0.19
MLA			−5.18 ± 0.05	−1.28 ± 0.15
Hexamethonium			−4.97 ± 0.07	−1.42 ± 0.25
Lobeline			−4.68 ± 0.07	−1.18 ± 0.20
Alcuronium			−4.59 ± 0.05	−1.26 ± 0.13
Vecuronium			−4.56 ± 0.03	−1.51 ± 0.15
d-Tubocurarine			−4.21 ± 0.07	−1.19 ± 0.19
Pancuronium			−4.04 ± 0.08	−1.04 ± 0.18
Eserine			−3.89 ± 0.05	−1.34 ± 0.19
Decamethonium			−3.52 ± 0.07	−1.24 ± 0.16
Succinylcholine			$\ll-3$	

TABLE 3

Parameters for interactions of indicated drugs with hα 4β 2-nAChR in transfected SH-EP1 cell**s.**

Results presented in Figs. 6–9 and in Tables 1 and 2 are summarized. Functional EC_{50} values for agonists, (column 2), functional IC_{50} values for antagonists (column 3; functional IC_{50} values given in parentheses for nicotine and suberyldicholine from fits to the self-inhibitory phase of agonist dose-response profiles for those drugs), and [^{3}H]EBDN binding competition K_i values (column 4), all in micromolar, are expressed to allow comparisons between functional and radioligand binding competition affinities for the indicated ligands (drug; column 1). Also indicated (F/B; column 5) is the ratio between the functional EC_{50}/IC_{50} and the binding competition K_i value (based on the IC_{50} value but corrected for the concentration of H-EBDN used in those assays and for the H-EBDN binding K_D of 10 pM using the Cheng-Prusoff correction) for each ligand. The notations after the drug name for selected ligands indicate, from results shown in Fig. 9, functional antagonism actions as a noncompetitive inhibitor (N), a competitive inhibitor (C), or a mixed competitive/noncompetitive inhibitor (N/C).

	Functional		Binding Competition	
Drug	EC_{50}	IC_{50}	(K_i)	F/B
	μM		μM	
Epibatidine	0.0085		0.000012	710
Nicotine	0.85	(5800)	0.0020	430
Cytisine	1.3		0.00024	5400
Suberyldicholine	1.3	360 (200)	0.013	100
ACh	1.7		0.018	94
DMPP	1.9		0.020	95
Carbamylcholine	17		0.15	110
Acetylthiocholine	100		0.17	590
Choline	~3800		7.0	>540
Lobeline		21	0.0019	11,000
Succinylcholine		$\gg$ 1000	2.9	>340
Decamethonium C		300	1.3	230
d-tubocurarine N/C		62	2.0	31
DHβE C	1.5	0.085	18	
MLA C	6.6	2.3	2.8	
Eserine N		130	>24	< 5.4
Vecuronium		28	24	1.2
Alcuronium		26	19	1.4
Pancuronium N/C		91	57	1.6
Hexamethonium N/C		11	45	0.24
Mecamylamine N		0.47	$\gg$24	< 0.02

With regard to functional properties of hα4β2-nAChR, high sensitivities to antagonism by mecamylamine or DHβE seem to be distinguishing characteristics, as are high sensitivities to agonist action of EBDN or nicotine. Ion flux assays indicate that choline has about 20 to 25% efficacy at 1 mM when acting at hα4β2-nAChR, meaning that its functional

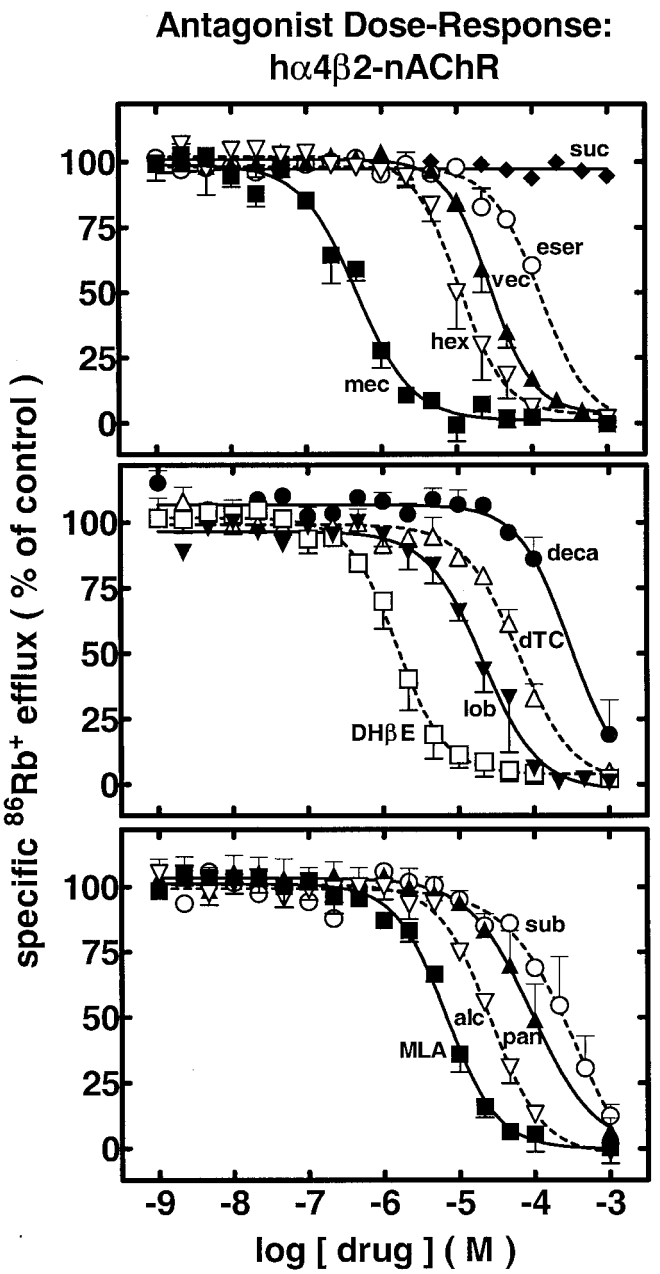

Fig. 8. Antagonist dose-response profiles for blockade of hα4β2-nAChR function. Specific $^{86}Rb^+$ efflux (ordinate; percentage of control) was determined in the presence of 1 mM carbamylcholine as described under *Materials and Methods* alone or in the presence of the indicated concentrations (abscissa; log molar scale) of: top, mecamylamine (mec; ■), hexamethonium (hexa; ▽), vecuronium (vec; ▲), eserine (eser; ○), or succinylcholine (suc; ♦); middle, DHβE (□), lobeline (lob; ▼), *d*-tubocurarine (dTC; △), or decamethonium (deca; ●); bottom, MLA (■), alcuronium (alc; ▽), pancuronium (pan; ▲), or suberyldicholine (sub; ○). Log IC_{50} values and Hill coefficients (± S.E.M.) are provided in Table 2, and functional IC_{50} values are indicated in the text and in Table 3. Maximum and minimum values for specific $^{86}Rb^+$ efflux obtained from curve fitting were 100 ± 5% or 0 ± 5%, respectively, of control values except for decamethonium (maximum of −107 ± 1% of control), and except for fits to the Hill equation for pancuronium, decamethonium, and eserine, which were based on minimum specific efflux values fixed at 0% of control.

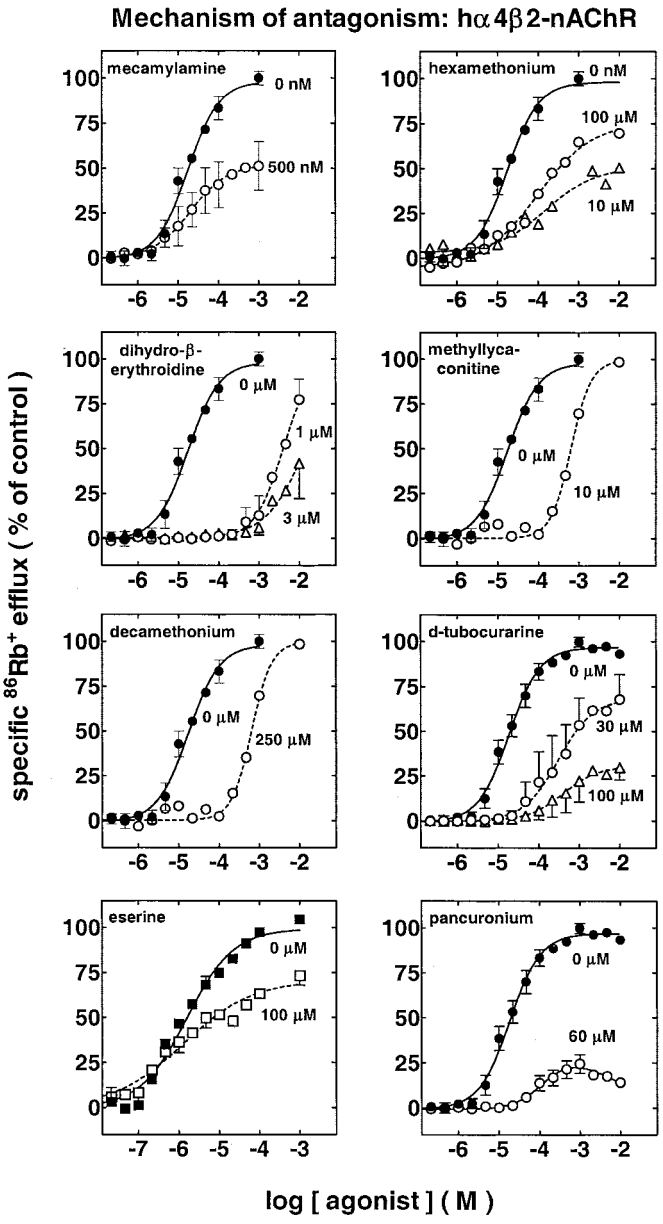

Fig. 9. Mechanisms of antagonist block of hα4β2-nAChR function. Specific $^{86}Rb^+$ efflux (ordinate; percentage of control) assays were done as described under *Materials and Methods* for samples challenged with the indicated dose (abscissa, log molar scale) of agonist alone (● for carbamylcholine, 98 ± 5% efficacy, −4.77 ± 0.08 log EC_{50}; ■ for ACh, 99 ± 3% efficacy, −5.80 ± 0.07 log EC_{50}) or of agonist in the presence of 500 nM mecamylamine (○; top left; 52 ± 6% efficacy, −4.70 ± 0.20 log EC_{50}), 100 μM hexamethonium (○; 76 ± 4% efficacy, −4.03 ± 0.08 log EC_{50}) or 10 μM hexamethonium (△; top right; 51 ± 4% efficacy, −3.83 ± 0.20 log EC_{50}), 1 μM dihydro-β-erythroidine (○; upper middle left; 99 ± 2% efficacy, −2.40 ± 0.06 log EC_{50}), 3 μM dihydro-β-erythroidine (△; upper middle left; fix at 100% efficacy, −1.84 ± 0.16 log EC_{50}), 10 μM methyllycaconitine (○; upper middle right; 99 ± 4% efficacy, −3.20 ± 0.04 log EC_{50}), 250 μM decamethonium (○; lower middle left; 102 ± 5% efficacy, −3.70 ± 0.07 log EC_{50}), 30 μM *d*-tubocurarine (○; lower middle right; 68 ± 6% efficacy, −3.52 ± 0.17 log EC_{50}), 100 μM *d*-tubocurarine (△; lower middle right; 31 ± 4% efficacy, −3.41 ± 0.21 log EC_{50}), 100 μM eserine (□; bottom left; 71 ± 4% efficacy, −5.90 ± 0.16 log EC_{50}), or 60 μM pancuronium (○; bottom right; 33 ± 47% efficacy, −3.88 ± 0.54 log EC_{50}). Carbamylcholine was the agonist used in all cases except for in studies using eserine, for which acetylcholine was the agonist.

potency at h$\alpha4\beta2$-nAChR is not very different from its potency at rat $\alpha7$-nAChR in hippocampal neurons (Albuquerque et al., 1998). Cytisine, DMPP, and suberyldicholine are partial agonists at h$\alpha4\beta2$-nAChR, and nicotine and suberyldicholine also exhibit self-inhibitory activity at higher doses. There was no convincing evidence for a two-site fit to agonist functional dose-response profiles, as has been seen by others using electrophysiological rather than ion flux assays and the HEK293 cell host instead of SH-EP1 cells (Buisson and Bertrand, 2001). Placement of constraints on curve fitting parameters did not yield two-site fits that were any better statistically than one-site fits, and the current results used comparatively dense, one-third log unit drug concentration profiles to derive those fits. The possibility of differences in host cell influences on properties of nAChR underscores the need to develop heterologous expression in different models but also indicates that studies in neurons of native nAChR will ultimately be required.

In contrast to the tight relationships between radioligand binding competition-derived K_i values for h$\alpha4\beta2$-nAChR expressed in two different mammalian cell hosts, comparisons of absolute functional agonist or antagonist potencies at heterologously expressed h$\alpha4\beta2$-nAChR expressed in different systems reveal some striking similarities or differences (Table 4). For example, membrane potential fluorescence-based measurements of agonist-activated, human $\alpha4\beta2$-nAChR function in transfected HEK cells (Fitch et al., 2003) give nearly perfect agreement with ion flux-based assays of agonist action at SH-EP1 cell-expressed human $\alpha4\beta2$-nAChR (this study; Table 4). EC_{50} values for EBDN and DMPP and IC_{50} values for the competitive antagonist, DHβE, agree within a factor of 2 for expression in SH-EP1 or HEK cells and for function measured using ion flux assays (Table 4; this study and Gopalakrishnan et al., 1996), although discrepancies are evident for nicotine, cytisine, and ACh. Whole-cell current recording from transfected HEK cells (Buisson et al., 1996) yields EC_{50} values for nicotine and ACh in good agreement with the SH-EP1 cell ion flux data (this study; Table 4), although there is a discrepancy for cytisine. Congruence of raw IC_{50} value data for competitive antagonists might not be expected, because agonist doses used relative to EC_{50} values often differ across studies. Moreover, the 4- to 20-fold difference in derived IC_{50} values for DHβE and MLA from this study and from Buisson et al. (1996) may be attributable to their analysis of the effects of antagonists on steady-state, partially desensitized currents rather than on time-integrated ion flux. However, an oocyte, whole-cell recording study (Chavez-Noriega et al., 1997) gives IC_{50} values for *d*-tubocurarine and DHβE that are 13- to 20-fold lower than those obtained in the current investigation (Table 4). Moreover, two different whole-cell recording studies using oocytes give 2- to 60-fold higher EC_{50} values for nicotinic agonists than determined in the current or other studies using cell line expression (Table 4), raising concern about how accurately studies of agonist potency at nAChR is when measured using the oocyte expression system. Nevertheless, rank order functional inhibitory potencies for antagonists are preserved across studies, as are rank-order potencies for EBDN, nicotine, and ACh. The agonists that fall out of rank order across studies are cytisine and DMPP, and perhaps this reflects their partial agonist actions at $\alpha4\beta2$-nAChR compounded by very different estimates of their efficacies across studies.

When contrasting functional and radioligand binding competition binding data, the initial intent was to assess usefulness of the approach to discriminate mechanisms of block for drugs acting on nAChR shuttling between states in a classic cyclic reaction scheme (e.g., basal inactivated to agonist-bound activated to agonist-bound desensitized and back to basal states). However, given the broad ranges of F/B functional affinity/binding affinity ratios within and across classes of agonists, competitive antagonists, and noncompetitive antagonists, the results seem to be more supportive of allosteric models in which a variety of channel-open or channel-closed states can exist and in which specific sets of states are stabilized by interactions with different drugs (Edelstein et al., 1996). Factored into this analysis are complicating issues such as differing abilities of agonists to induce short-term loss of nAChR function (i.e., during milliseconds or seconds of drug exposure), with longer-lasting exposure (e.g., for the min of exposure used for $^{86}Rb^+$ flux assays), or with more long-term exposure (minutes/hours). Moreover, preliminary electrophysiological studies indicate that antagonists can differentially affect peak or steady state whole-cell currents induced by agonists (Wu et al., 2001), perhaps consistent with different affinities for open, closed, and/or desensitized states. Perhaps systematic studies and their analyses, as attempted in the present report will help guide efforts to approaches useful in discriminating different allosteric

TABLE 4

Comparisons of functional EC_{50} or IC_{50} values for human α 4β2-nAChR expressed in different systems.

Functional EC_{50} values for agonists or functional IC_{50} values for antagonists (all in micromolar) are summarized for studies examining human α 4β2-nAChR heterologously expressed in human SH-EP1 or HEK cells or in oocytes and assessed using $^{86}Rb^+$ efflux assays, membrane potential fluorescence (V_m fluor), or whole-cell current recording (e'phys) as indicated.

Drug	This Study SH-EP1 $^{86}Rb^+$ efflux	Buissonet al., 1996 HEK e'phys	Gopalakrishnan et al., 1996 HEK $^{86}Rb^+$ efflux	Fitch et al., 2003 HEK V_m fluor	Chavez Noriegaet al., 1997 Oocyte e'phys	Papke et al., 2000 Oocyte e'phys
Epibatidine	0.0085	N.R.	0.017	0.0053	N.R.	N.R.
Nicotine	0.85	1.6	4.0	0.86	5.5	52
Cytisine	1.3	12	38	1.7	2.6	N.R.
ACh	1.7	3.0	44	N.R.	68	92
DMPP	1.9	N.R.	2.5	2.2	18	N.R.
DHβE[a]	1.5	0.08[b]	1.9	25	0.11	N.R.
MLA[a]	6.6	1.5[b]	N.R.	N.R.	N.R.	N.R.
d-Tubocurarine[a]	62	N.R.	N.R.	N.R.	3.2	N.R.

N.R., not reported.

[a] Antagonists.

[b] Values indicated were obtained not from blockade of whole-cell peak currents but from blockade of steady-state currents after part of the whole-cell response had desensitized.

states of nAChR. Nevertheless, the current studies may indicate that antagonist and epibatidine binding sites on h$\alpha\beta$2-nAChR have little-to-no physical overlap or that these ligands stabilize hα4β2-nAChR conformations that have negligible affinity for the heterologous class of ligands.

Acknowledgments

We thank Dr. June Biedler and Barbara Spengler for SH-EP1 cells and Dr. Lynn Wecker (University of South Florida) for alerting us to α4 subunit sequence differences relative to the reference sequence.

References

Abood LG and Grassi S (1986) [^{3}H]Methylcarbamylcholine, a new radioligand for studying brain nicotinic receptors. *Biochem Pharmacol* **35:**4199–4202.

Albuquerque EX, Alkondon M, Pereira EFR, Castro NG, Schrattenholz A, Barbosa CTF, Bonfante-Cabarcas R, Aracava Y, Eisenberg HM, and Maelicke A (1998) Properties of neuronal nicotinic acetylcholine receptors: Pharmacological characterization and modulation of synaptic activity. *J Pharmacol Exp Ther* **280:**1117–1136.

Alexander SPH and Peters JA (2001) eds. Receptor Ion Channel Nomenclature Supplement, *Trends Pharmacol Sci* **22**(Suppl)**:**7–12.

Alkondon M and Albuquerque EX (1993) Diversity of nicotinic acetylcholine receptors in rat hippocampal neurons. I. Pharmacological and functional evidence for distinct structural subtypes. *J Pharmacol Exper Ther* **265:**1455–1473.

Alkondon M and Albuquerque EX (1995) Diversity of nicotinic acetylcholine receptors in rat hippocampal neurons. III. Agonist actions of the novel alkaloid epibatidine and analysis of type II current. *J Pharmacol Exp Ther* **274:**771–782.

Bencherif M and Lukas RJ (1993) Cytochalasin modulation of nicotinic cholinergic receptor expression and muscarinic receptor function in human TE671/RD cells: a possible functional role of the cytoskeleton. *J Neurochem* **61:**852–864.

Buisson B, Gopalakrishnan M, Arneric SP, Sullivan JP, and Bertrand D (1996) Human α4β2 neuronal nicotinic acetylcholine receptors in HEK 293 cells: a patch-clamp study. *J Neurosci* **16:**7880–7891.

Buisson B and Bertrand D (2001) Chronic exposure to nicotine upregulates the human α4β2 nicotinic acetylcholine receptor function. *J Neurosci* **21:**1819–1829.

Buisson B, Vallejo YF, Green WN, and Bertrand D (2000) The unusual nature of epibatidine responses at the alpha4beta2 nicotinic acetylcholine receptor. *Neuropharmacol* **39:**2561–2569.

Chavez-Noriega LE, Crona JH, Washburn MS, Urrutia A, Elliott KJ, and Johnson EC (1997) Pharmacological characterization of recombinant human neuronal nicotinic acetylcholine receptors hα2β2, hα2β4, hα3β2, hα3β4, hα4β2, hα4β4 and hα7 expressed in *Xenopus* oocytes. *J Pharmacol Exp Ther* **280:**346–356.

Clementi F, Fornasari D, and Gotti C (2000), eds. *Neuronal Nicotinic Receptors*. Handbook of Experimental Pharmacology, Vol 144, Spinger-Verlag, Heidelberg.

Cooper ST, Harkness PC, Baker ER, and Millar NS (1999) Up-regulation of cell-surface α4β2 neuronal nicotinic receptors by lower temperature and expression of chimeric subunits. *J Biol Chem* **274:**27145–27152.

Cordero-Erausquin M, Marubio LM, Klink R, and Changeux J-P (2000) Nicotinic receptor function: perspectives from knockout mice. *Trends Pharmacol Sci* **21:**211–217.

Davila-Garcia MI, Musachio JL, Perry DC, Xiao Y, Horti A, London ED, Dannals RF, and Kellar KJ (1997) [^{125}I]IPH, an epibatidine analog, binds with high affinity to neuronal nicotinic cholinergic receptors. *J Pharmacol Exp Ther* **282:**445–451.

Eaton JB, Kuo Y-P, Fuh LP-t, Krishnan C, Steinlein O, Lindstrom JM, Lukas RJ (2000) Properties of stably and heterologously-expressed human α4β4-nicotinic acetylcholine receptors (nAChR). *Soc Neurosci Abst* **26:**371.

Edelstein SJ, Schaad O, Henry E, Bertrand D, and Changeux J-P (1996) A kinetic mechanism for nicotinic acetylcholine receptors based on multiple allosteric transitions. *Biol Cybernet* **75:**361–379.

Elgoyhen AB, Vetter DE, Katz E, Rothlin CV, Heinemann SF, and Boulter J (2001) α10: A determinant of nicotinic cholinergic receptor function in mammalian vestibular and cochlear mechanosensory hair cells. *Proc Natl Acad Sci USA* **98**:3501–3506.

Elliott KJ, Ellis SB, Berckhan KJ, Urrutia A, Chavez-Noriega LE, Johnson EC, Velicelebi G, and Harpold MM (1996) Comparative structure of human neuronal α2-α7 and β2-β4 nicotinic acetylcholine receptor subunits and functional expression of the α2, α3, α4, α7, β2 and β4 subunits. *J Mol Neurosci* **7:**217–228.

Fenster CP, Rains MF, Noerager B, Quick MW, and Lester RA (1997) Influence of subunit composition on desensitization of neuronal acetylcholine receptors at low concentrations of nicotine. *J Neurosci* **17:**5747–5759.

Ferchmin PA, Lukas RJ, Hann RM, Fryer JD, Eaton JB, Pagan OR, Rodriguez AD, Nicolau Y, Rosado Y, Cortes S, et al. (2001) Tobacco cembranoids block behavioral sensitization to nicotine and inhibit neuronal acetylcholine receptor function. *J Neurosci Res* **64:**18–25.

Fitch RW, Xiao Y, Kellar KJ, and Daly JW (2003) Membrane potential fluorescence: a raid and highly sensitive assay for nicotinic receptor channel function. *Proc Natl Acad Sci USA* **100:**4909–4914.

Flores CM, Rogers SW, Pabreza LA, Wolfe BB, and Kellar KJ (1992) A subtype of nicotinic cholinergic receptor in rat brain is composed of α4 and β2 subunits and is up-regulated by chronic nicotine treatment. *Mol Pharmacol* **41:**31–37.

Gopalakrishnan M, Monteggia LM, Anderson DJ, Molinari EJ, Iattoni-Kaplan M, Donnelly-Roberts D, Arneric SP, and Sullivan JP (1996) Stable expression, pharmacologic properties and regulation of the human neuronal nicotinic acetylcholine α4β2 receptor. *J Pharmacol Exp Ther* **276:**289–297.

Gopalakrishnan M, Molinari EJ, and Sullivan JP (1997) Regulation of human α4β2 neuronal nicotinic acetylcholine receptors by cholinergic channel ligands and second messenger pathways. *Mol Pharmacol* **52:**524–534.

Houghtling RA, Davila-Garcia MI, Hurt SD, and Kellar KJ (1994) [^{3}H]Epibatidine binding to nicotinic cholinergic receptors in brain. *Med Chem Res* **4:**538–546.

Houghtling RA, Davila-Garcia MI, and Kellar KJ (1995) Characterization of (±)-[^{3}H]Epibatidine binding to nicotinic cholinergic receptors in rat and human brain. *Mol Pharmacol* **48:**280–287.

Lindstrom J (1996) Neuronal nicotinic acetylcholine receptors. In: *Ion Channels*, Vol 4 (Narahashi T ed) pp 377–450, New York, Plenum Press.

Lukas RJ (1986) Characterization of curaremimetic neurotoxin binding sites on membrane fractions derived from the human medulloblastoma clonal line, TE671. *J Neurochem* **46:**1936–1941.

Lukas RJ (1990) Heterogeneity of high-affinity nicotinic [^{3}H]acetylcholine binding sites. *J Pharmacol Exp Ther* **253:**51–57.

Lukas RJ (1998) Neuronal nicotinic acetylcholine receptors. In: *The Nicotinic Acetylcholine Receptor: Current Views and Future Trends* (Barrantes FJ ed), pp 145–173, Springer-Verlag, Berlin.

Lukas RJ, Norman SA, and Lucero L (1993) Characterization of nicotinic acetylcholine receptors expressed by cells of the SH-SY5Y human neuroblastoma clonal line. *Mol Cell Neurosci* **4:**1–12.

Lukas RJ, Changeux J-P, Le Novère N, Albuquerque EX, Balfour DJK, Berg DK, Bertrand D, Chiappinelli VA, Clarke PBS, Collins AC, et al. (1999) International Union of Pharmacology. XX. Current status of the nomenclature for nicotinic acetylcholine receptors and their subunits. *Pharmacol Rev* **51:**397–401.

Lukas RJ, Fryer JD, Eaton JB, and Gentry CL (2002) Some methods for studies of nicotinic acetylcholine receptor pharmacology, in *Nicotinic Receptors and the Nervous System* (Levin ED ed) pp 3–27, Boca Raton, CRC Press.

Marks MJ and Collins AC (1982) Characterization of nicotine binding in mouse brain and comparison with the binding of α-bungarotoxin and quinuclidinyl benzilate. *Mol Pharmacol* **22:**554–564.

Pabreza LA, Dhawan S, and Kellar KJ (1991) [^{3}H]Cytisine binding to nicotinic cholinergic receptors in brain. *Mol Pharmacol* **39:**9–12.

Pacheco MA, Pastoor TE, Lukas RJ, and Wecker L (2001) Characterization of human α4β2 neuronal nicotinic receptors stably expressed in SH-EP1 cells. *Neurochem Res* **23:**683–693.

Papke RL, Webster JC, Lippiello PM, Bencherif M, and Francis MM (2000) The activation and inhibition of human nicotinic receptor by RJR-2403 indicate a selectivity for the α4β2 receptor subtype. *J Neurochem* **75:**204–216.

Peng J-H, Eaton JB, Eisenhour CM, Fryer JD, Lucero L, and Lukas RJ (1999) Properties of stably and heterologously-expressed human α4β2-nicotinic acetylcholine receptors (nAChR). *Soc Neurosci Abst* **25:**172319.

Picciotto MR, Zoli M, Lena C, Bessis A, Lallemand Y, Le Novere N, Vincent P, Pich EM, Brulet P, and Changeux J-P (1995) Abnormal avoidance learning in mice lacking functional high-affinity nicotine receptor in the brain. *Nature (Lond)* **374:**65–67.

Rempel N, Heyers S, Engels H, Sleegers E, and Steinlein OK (1998) The structures of the human neuronal nicotinic acetylcholine receptor beta2- and alpha3-subunit genes (CHRNB2 and CHRNA3). *Hum Genet* **103:**645–853.

Romano C and Goldstein A (1980) Stereospecific nicotine receptors on rat brain membranes. *Science (Wash DC)* **210:**647–649.

Ross RA, Spengler BA, and Biedler JL (1983) Coordinate morphological and biochemical interconversion of human neuroblastoma cells. *J Natl Cancer Inst* **71:**741–747.

Schwartz RD, McGee R, and Kellar KJ (1982) Nicotinic cholinergic receptors labeled by acetylcholine in rat brain. *Mol Pharmacol* **2:**56–62.

Shafaee N, Houng M, Truong A, Viseshakul N, Figl A, Sandhu S, Forsayeth JR, Dwoskin LP, Crooks PA, and Cohen BN (1999) Pharmacological similarities between native brain and heterologously expressed α4β2 nicotinic receptors. *Br J Pharmacol* **128:**1291–1299.

Steinlein OK (2001) Genes and mutations in idiopathic epilepsy. *Am J Med Genet* **106:**139–145.

Steinlein O, Weiland S, Stoodt J, and Propping P (1996) Exon-intron structure of the human neuronal nicotinic acetylcholine receptor α4 subunit (CHRNA4). *Genomics* **32:**289–294.

Whiting PJ and Lindstrom J (1987) Purification and characterization of a nicotinic acetylcholine receptor from rat brain. *Proc Natl Acad Sci USA* **84:**595–599.

Wu J, Segerberg M, Peng J-H, Kuo Y-P, Eaton JB, and Lukas RJ (2001) Acute desensitization of heterologously expressed human α4β2-nicotinic receptors. *Soc Neurosci Abst* **27:**380.

Whiting P, Schoepfer R, Lindstrom J, and Priestley T (1991) Structural and pharmacological characterization of the major brain nicotinic acetylcholine receptor subtype stably expressed in mouse fibroblasts. *Mol Pharmacol* **40:**463–472.

Address correspondence to: Dr. Ronald J. Lukas, Division of Neurobiology, Barrow Neurological Institute, 350 West Thomas Road, Phoenix, Arizona 85013. E-mail: rlukas@chw.edu